Theor Chem Acc (1999) 101:209–214
DOI 10.1007/s00214980m109

Theoretical
Chemistry Accounts

Regular article

Why betaine crystallizes in high local C_s symmetry. An ab initio MO and DFT study of anhydrous betaine and betaine monohydrate*

Tommi H. Nyrönen[1], **Reijo Suontamo**[2], **Ilkka Pitkänen**[2]

[1] CSC – Center for Scientific Computing, P.O. Box 405, FIN-02101 Espoo, Finland
[2] Department of Chemistry, University of Jyväskylä, P.O. Box 35, FIN-40351 Jyväskylä, Finland

Received: 24 March 1998 / Accepted: 3 September 1998 / Published online: 7 December 1998

Abstract. A theoretical study of the structure, charge distribution, rotational barrier and fundamental vibrations of anhydrous betaine $(CH_3)_3NCH_2COO$ (trimethylglycine) was carried out and compared with available experimental data. Calculations were carried out at HF, MP2 and B3LYP levels using a 6-31+G(*d,p*) basis set. The calculated rotational barrier of the betaine carboxylic group is 40.5 kJ/mol at the MP4(SDQ)/6-311G(*d,p*)//HF/6-31+G(*d,p*) level of theory. The rotation of the carboxylic group changes the molecule from a highly symmetric (C_s) conformation into a twisted conformation resulting in shortening of the molecule by about 50 pm. Natural population analysis (NPA) indicates intramolecular interaction between the carboxylic oxygen and the nearest methyl hydrogens resulting in internal hydrogen bonding. MP4(SDQ)/6-311G(*d,p*) single-point NPA calculations on a betaine monohydrate model taken from the X-ray geometry show an expected weakening in the internal hydrogen bond. Calculations explain why betaine preferentially crystallizes in high local C_s symmetry.

Key words: Ab initio molecular orbital and density functional theory calculations – Trimethylglycine – Anhydrous betaine – Betaine monohydrate – Charge distribution – Rotational barrier

1 Introduction

Betaine compounds are commonly zwitterionic with two formally charged substituent groups that are not conjugated. Because of their polar nature, betaines form complexes with several organic and inorganic chemical substances [1–3]. Betaines occur naturally in molasses and are biologically important. They are found in complex lipids, in metabolic systems and as transmethylating agents. In cells betaine binds water molecules and assists in controlling the osmotic pressure [4]. Betaine hydrochloride, $((CH_3)_3NCH_2COOH)Cl$, has been added to commercial products such as bath and shower gels and vitamin pills. Food and Drug Administration officials in the USA have recently declared anhydrous betaine as a drug.

The crystal structure and the IR spectrum of anhydrous betaine, $(CH_3)_3NCH_2COO$, [5] and betaine monohydrate, $(CH_3)_3NCH_2COOH_2O$, [6] are known. In both crystalline forms the betaine molecule possess C_s local symmetry [5, 6]. This might be a result of some interaction, maybe weak internal hydrogen bonding, between groups of different polarity. Inspecting the geometry of the betaine molecule indicates that the carboxylic group can rotate with respect to the C—C bond adjacent to it. This might assist the molecule to penetrate cell walls.

In betaine monohydrate, carboxylic oxygens are both hydrogen-bonded to different water molecules [6], and this should reduce the polarity of the betaine molecule. The carboxylic oxygens of the anhydrous form are not bonded to other molecules [5]. An interesting question arises: Is there a weak intramolecular hydrogen bond between the positive methyl group hydrogens and the negative carboxylic oxygens in betaine and if there is, is it different in magnitude in anhydrous and monohydrate forms? Details of intramolecular hydrogen bonding and charge distribution of anhydrous betaine and betaine monohydrate should provide an insight into reaction mechanisms of the molecule. Possible internal hydrogen bonding could be used to explain why the C_s symmetry is so highly conserved in the crystallization process of anhydrous betaine.

Lower-level ab initio studies on anhydrous betaine have previously been carried out by Latajka and Ratajczak [7]. No theoretical calculations have been reported on betaine monohydrate.

---

*Contribution to the Proceedings of Computational Chemistry and the Living World, April 20–24, 1998, Chambery, France

Correspondence to: T.H. Nyrönen
e-mail: tommi.nyronen@csc.fi

2 Calculations

The starting geometry for a more comprehensive geometry optimization of anhydrous betaine was obtained using the semiempirical PM3 method [8, 9] implemented in the HyperChem program [10]. The calculations were made using the Gaussian 94 package [11], utilizing the standard 6-31+G(*d*,*p*) [12] basis set which was used throughout unless noted otherwise. Geometry optimizations were first done at the Hartree-Fock (HF) level of theory with gradient techniques. Effects of dynamic electron correlation on the geometries were investigated by optimizing the geometries according to Becke's three parameter hybrid method with the Lee, Yang and Parr correlation functional (B3LYP) [13–15] and second-order Møller–Plesset perturbation theory (MP2) [16–19]. The fundamental vibrations of the ground-state geometry were calculated at the HF and B3LYP levels of theory.

The carboxylic group rotational barrier of anhydrous betaine was estimated by fixing the C2—N1—C4—C5 torsion angle (see Figs. 1, 2) to values of 0, 30 and 60 degrees and allowing the structure to relax at the HF level with respect to all other structural parameters. A HF frequency calculation was carried out for each structure to establish the nature of the stationary points. The energies of the stationary points were calculated at the HF/6-31+(*d*,*p*) and MP4(SDQ)/6-311G(*d*,*p*)//HF/6-31+G(*d*,*p*) levels to approximate the height of the carboxylic rotational barrier.

In order to evaluate the atomic charges several approaches were considered in addition to standard Mulliken population analysis. Natural population analysis (NPA) calculations were carried out at MP2 level to evaluate partial charges for three different conformations of anhydrous betaine involved in the carboxylic group rotation and for the betaine monohydrate model extracted from the crystal structure [6]. The NPA approach was compared to other methods that are available for partial charge calculation by fitting the charges to the electrostatic potential derived from the MP2 wavefunction of the C_s symmetric anhydrous betaine (Fig. 1) according to the CHELPG scheme of Breneman and Wiberg [23] and to the Merz-Singh-Kollman scheme (MK) [24, 25]. Visualizations were carried out using WebLab Viewer [26] and POV-Ray [32].

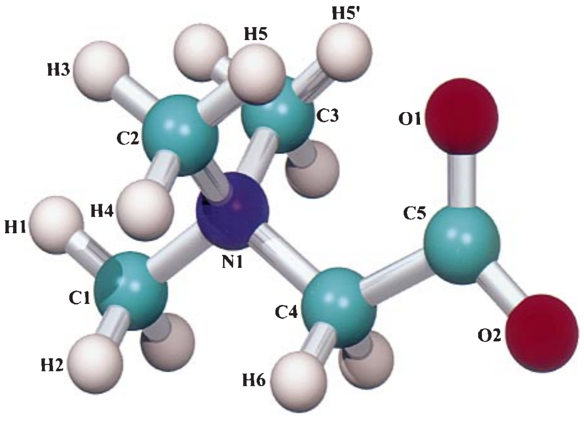

Fig. 1. Structure and labeling of atoms in anhydrous betaine. The molecule has C_s local symmetry

3 Results and discussion

Geometry

The optimum geometry and the labeling of atoms in C_s symmetric anhydrous betaine are presented in Fig. 1. This lowest energy ground-state geometry is also depicted in Fig. 2a. The same scheme of labeling is used in the model of betaine monohydrate (see Fig. 3). The experimental and calculated bond lengths, bond angles and selected torsion angles are summarized in Table 1. Our results are in fair agreement with earlier ab initio calculations [7].

There is a striking similarity in the experimental betaine molecule structure both in the hydrogen-bonded environment and in the anhydrous state with no hydrogen bonds (see Table 1). The optimized ground-state geometries of anhydrous betaine at the HF, B3LYP and MP2 levels all predict the experimental X-ray geometry reasonably well. C_s symmetric anhydrous betaine is established as the lowest energy state with HF, MP2 and B3LYP methods. There is, however, notable disagreement in the hydrogen bond lengths. This is due to the X-ray structure determination method underestimating the distances of bonded hydrogens [5]. All the other calculated structural parameters are in agreement with the X-ray molecular structure of anhydrous betaine. Szafran and Koput [27] found that in the case of pyridine betaine the introduction of dynamic electron-correlation methods resulted in longer bonds and poorer agreement with the experimental geometry. Geometry optimization with methods using electron correlation (MP2, B3LYP) results in slight overestimation of bond lengths, as expected, especially for N1—C4, C4—C5 and C5—O1 bonds. The C=O bond length is known to be hard to model. In their study of the internal rotation of acetaldehyde, Goodman et al. [28] pointed out that the MP2/6-311+G(3*df*,2*p*) level was needed to produce the correct C=O bond length. Bond angles calculated at MP2 and B3LYP levels also differ more from the experimental values than those calculated at HF level. Especially the O1—C5—O2 bond angle is overestimated by all methods. In this study, however, the changes in geometry produced by optimization with electron-correlation methods are small and do not lead to significantly different conformations.

The experimental C_s molecular symmetry of betaine, both in anhydrous and monohydrate form, might be in part due to weak three-center intramolecular hydrogen bonding between the carboxylic oxygen O1 and the hydrogens H5 and H5′ of the nearest methyl groups. The experimental distance O1-H5 of 237.2 pm [5] in anhydrous betaine and 238.7 pm [6] in the monohydrate are indeed both well below the cut-off value of 285 pm for a hydrogen bond in sugars [29]. The calculated O1-H5 distances are even less, 219.1–213.7 pm. The O1-H5 distance is only 0.5 pm shorter in the anhydrous form, a

Fig. 2a–c. Rotation of the carboxylic group in anhydrous betaine. **a** C_s symmetric ground-state structure, C5—C4—N1—C2 torsion angle 60°. **b** Local-minimum structure, C5—C4—N1—C2 torsion angle 30°. **c** Transition-state structure, C5—C4—N1—C2 torsion angle 0°

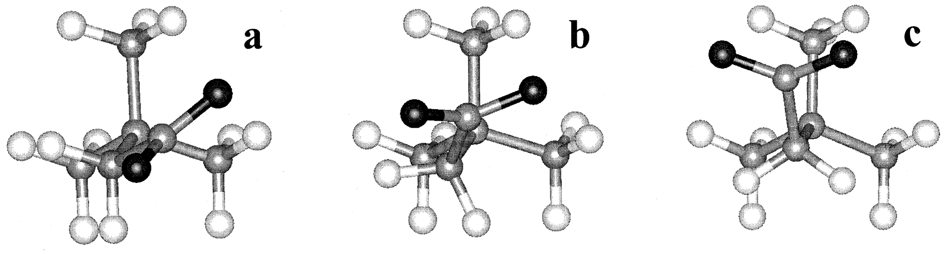

C_s symmetric ground state
E[HF] = -399.900912 a.u.
E[MP4] = - 401.356280 a.u.

Local minimum
E[HF] = -399.895010 a.u.
E[MP4] = -401.349929 a.u.
ΔE[HF] = 0.005902 a.u.
ΔE[MP4]= 0.006351 a.u.

Transition state
E[HF] = -399.886715 a.u.
E[MP4] = - 401.340861 a.u.
ΔE[HF] = 0.014197 a.u.
ΔE[MP4] = 0.015419 a.u.

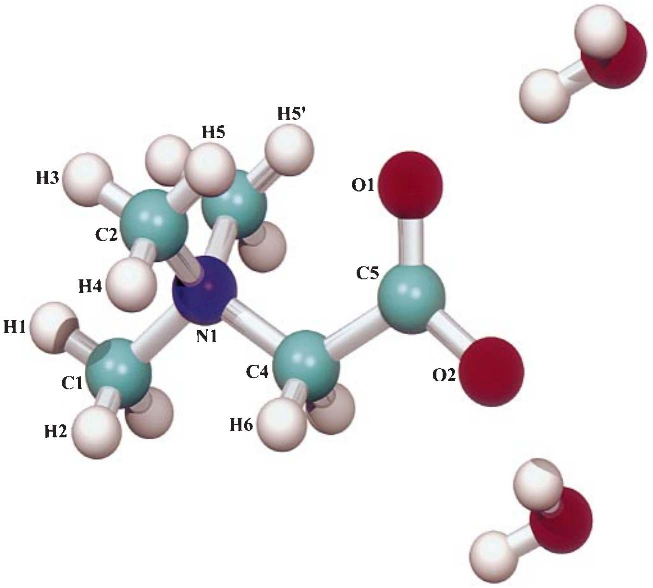

Fig. 3. Betaine monohydrate model used in the calculations. The structure is taken from Ref. [6]

difference which is of the order of the experimental error (±0.3 pm) [5]. On the other hand, the possible weak hydrogen bonding should lengthen the C2—H5 bond compared to the C2—H3 and C2—H4 bonds. As seen in Table 1, the calculated and experimental values of those bond lengths do not differ significantly. The longer C5—O1 bond compared to the C5—O2 bond might be another structural indication of a weak intramolecular hydrogen bond. The calculated and experimental lengths of the C5—O1 and C5—O2 bonds, however, do not differ significantly.

Rotational barrier of the carboxylic group

Three different structures were optimized at HF level to estimate the rotational barrier of anhydrous betaine: The ground state with the C5—C4—N1—C2 torsion angle fixed at 60° (Figs. 1, 2a), 30° (Fig. 2b), and 0° (Fig. 2c). Anhydrous betaine has a C_s symmetric ground-state structure as confirmed by the frequency calculation (all frequencies positive). The transition state, with the C5—C4—N1—C2 torsion angle fixed at 0°, was found to be a first-order transition state (one imaginary frequency). The intermediate structure with torsion angle 30° is a local minimum (all calculated frequencies are positive).

MP4(SDQ)/6-311G(*d,p*) single-point energy calculations were carried out with HF optimized structures. The eclipsed transition state is 0.014197 a.u. (37.3 kJ/mol) above the ground state at the HF/6-31+G(*d,p*) level and 0.015419 a.u. (40.5 kJ/mol) above the ground state at the MP4(SDQ)/6-311G(*d,p*)//HF/6-31+G(*d,p*) level. The intermediate state is 0.005902 a.u. (15.5 kJ/mol) above the ground state at the HF level and 0.006351 a.u. (16.7 kJ/mol) at the MP4(SDQ)/6-311G(*d,p*)//HF/6-31+G(*d,p*) level. This rotational barrier is rather high for a single C—C bond rotation (compared to 12.1 kJ/mol in ethane) [31]. This might in part be due to the extra energy needed to break the weak internal hydrogen bond during rotation. A graphical presentation of the energy profile along the C5—C4—N1—C2 torsion angle is presented in Fig. 4. A rotation of 120° returns the molecule to the initial position.

When anhydrous betaine is in its eclipsed transition geometry, the length of the molecule from O1 or O2 to the most distant hydrogen atom is reduced from 566.6 pm to 520.2 pm. The largest width of the molecule stays at a constant value of 417.5 pm. The rotation of the carboxylic group thus shortens the molecule by almost 50 pm. In the transition state the two hydrogen bonds stabilizing the C_s symmetric ground state between O1—H5 and O1—H5′ are broken. This interaction is replaced by two identical weaker O—H interactions between O1—H5 and O2—H4 (see Tables 1, 2). The O1—H5 distance is increased by 31.4 pm compared to the ground-state HF structure. In the intermediate structure the O1—H5 and O1—H5′ distances are similar to those in the ground-state structure but the energy of the conformation is higher due to the strained geometry. The transition-state geometry is still rather low in energy and might be easily reached in solution to assist betaine molecules to penetrate plant cell walls more efficiently.

Table 1. Selected structural parameters for betaine monohydrate, and anhydrous betaine conformations: ground state (1); intermediate (2); transition state (3)[a]

Parameter	Betaine monohydrate Experimental[b]	Anhydrous betaine Experimental[c]	Optimization method				
			HF (1)	B3LYP (1)	MP2 (1)	(2)	(3)
Bond lengths (pm)							
N1—C1	149.9	150.5	148.5	149.8	149.2	148.2	148.7
N1—C2	149.5	149.8	149.5	150.7	149.9	149.9	150.2
N1—C3	149.1	149.8	149.5	150.7	149.9	149.5	148.7
N1—C4	150.8	150.5	151.8	154.1	152.3	152.7	154.4
C4—C5	153.3	153.4	156.7	158.2	157.1	156.4	156.2
C5—O1	123.9	124.2	123.1	125.7	126.5	123.4	122.6
C5—O2	125.1	123.8	121.6	123.9	124.9	121.7	122.6
C1—H1	96.0	101.3	108.1	109.2	108.8	108.1	108.2
C1—H2	95.9	102.0	108.0	109.1	108.7	108.1	108.0
C2—H3	96.0	103.3	108.2	109.2	108.8	108.2	108.1
C2—H4	96.0	97.7	108.1	109.1	108.8	108.1	107.8
C2—H5	96.0	100.7	107.6	109.1	108.6	107.5	107.8
C4—H6	95.9	102.0	108.1	109.2	109.0	108.1	107.8
O1—H5	238.7	237.2	219.1	215.0	213.7	218.5	250.5
Bond angles (deg.)							
C1—N1—C2	108.3	108.0	108.9	109.4	109.1	109.7	108.1
C4—N1—C1	107.8	107.5	108.5	109.2	108.9	109.2	109.1
C3—N1—C1	108.2	108.0	108.9	109.4	109.1	109.6	109.7
C4—N1—C2	110.4	111.6	110.4	109.7	109.9	112.2	112.9
C3—N1—C2	110.7	109.9	109.6	109.5	109.7	107.4	108.1
C4—N1—C3	111.4	111.6	110.4	109.7	109.9	108.6	109.1
N1—C4—C5	117.6	118.4	117.3	117.0	116.8	114.5	111.1
C4—C5—O1	120.1	120.1	116.9	117.1	117.2	113.3	113.7
C4—C5—O2	112.6	111.9	110.5	110.3	110.1	114.1	113.7
O1—C5—O2	127.2	128.0	132.7	132.5	132.7	132.5	132.5
H1—C1—H2	109.5	110.0	109.7	109.9	110.2	109.8	109.8
H1—C1—N1	109.2	110.4	109.4	109.3	109.0	109.4	109.4
H2—C1—N1	109.7	107.5	109.3	109.1	108.7	109.1	109.2
H3—C2—H4	109.4	110.0	109.8	110.1	110.3	109.9	111.1
H3—C2—N1	109.4	110.0	108.5	108.6	108.3	108.0	107.8
H4—C2—H5	109.5	107.5	110.4	110.7	110.9	109.6	109.1
H4—C2—N1	109.7	108.3	108.4	108.3	107.9	108.6	108.8
H5—C2—N1	109.4	109.5	108.2	107.0	107.0	108.7	108.8
H6—C4—C5	107.5	109.3	108.7	109.2	109.2	110.4	110.7
Torsion angles (deg.)							
C1—N1—C4—C5	179.1	180.0	180.0	180.0	180.0	−151.9	−120.1
C2—N1—C4—C5	−62.8	−61.7	−60.7	−60.2	−60.5	−30.0	0.0
N1—C4—C5—O1	−2.3	0.0	0.0	0.0	0.0	−45.5	−88.3
N1—C4—C5—O2	177.4	180.0	180.0	180.0	180.0	135.9	88.3
H2—C1—N1—C2	−50.0	−60.3	−60.2	−60.2	−60.3	−177.2	−59.4
H4—C2—N1—C4	−58.1	−58.2	−60.2	−59.0	−53.2	−53.8	30.2
H6—C4—C5—O2	56.2	59.5	59.0	59.4	59.5	−103.4	−153.3

[a] For numbering of the atoms see Figs. 1 and 3

[b] From Ref. [6]

[c] From Ref. [5]

Charge distribution

The molecular charge distributions of anhydrous betaine and betaine monohydrate are presented in Tables 2 and 3. All the present methods indicate that the positive charge of the quaternary ammonium moiety is distributed rather evenly on the methyl hydrogen atoms. The NPA and Mulliken charges on the nitrogen atom are negative. On the other hand, fitting the electrostatic potential according to CHELPG and MK schemes, which are directed to accurately produce molecular properties such as dipole moments, suggests that the nitrogen atom is positive. The discrepancy between the methods is probably because the nitrogen atom is located within the molecule frame. The NPA of Reed et al. [21] is used to compare the charge distributions to make a possible discrimination among the various structures in terms of internal interactions. NPA creates natural atomic orbitals (NAOs) which are intrinsic to the wavefunction: NAOs converge as the wavefunction is improved. NPA has been used to discuss inter- and intramolecular interactions (for a review see Ref. [22]).

The zwitterionic polar nature of the betaine molecule should be reflected as differences between the calculated charges of methyl group hydrogens H3, H4 and H5, expecting the order $Q(\mathrm{H3}) > Q(\mathrm{H4}) > Q(\mathrm{H5})$. As seen in

Table 3, the calculated order is $Q(\mathrm{H5}) > Q(\mathrm{H4}) > Q(\mathrm{H3})$ for both forms, opposite to that expected on the grounds of the polar nature. Q(H5) being more positive suggests a partial intramolecular charge transfer from H5 to O1, which is thus more negative than O2. These NPA charges for H3, H4 and H5 in the anhydrous form are clearly more positive than in the monohydrate. O2 draws charge from hydrogen-bonded water molecules in the monohydrate model resulting in a more negative O2 charge than the in anhydrous form. O1 has nearly the same charge in both forms. The absolute value of the charge difference between O1 and H5 is 1.017 a.u. in the monohydrate and 1.058 a.u. in the anhydrous form. The three-center electronic interaction between O1 and H5 and H5′, as suggested by the atomic charges, is weakened when betaine oxygens are bonded outside the molecule. This weakening is reflected in the crystal structures as a change of O1—H5 distance from 237.2 pm [5] in anhydrous betaine to 238.7 pm in the monohydrate.

The rotation of the carboxylic group changes the natural charges of H4 and H5 (H5') as suggested by the changes in geometry. In the transition-state structure the natural charges of H4 and H5 are equal. O1 and O2 also carry identical charges in the transition state. The transition-state structure thus possesses high C_s symmetry in terms of geometrical parameters and charge distribution but is notably higher in energy than the ground-state structure.

The discussion of charges up to this point has been limited only to NPA charges, which seem to be capable of reflecting hydrogen bonding [22]. The Mulliken atomic charges give the same overall trends as NPA charges, but they do not produce the same charge distribution in the betaine molecule. CHELPG and MK schemes are not suitable for this kind of discussion on betaine internal hydrogen bonding.

Fundamental vibrations

Fundamental vibrations were calculated primarily to evaluate the nature of the stationary points. Experimen-

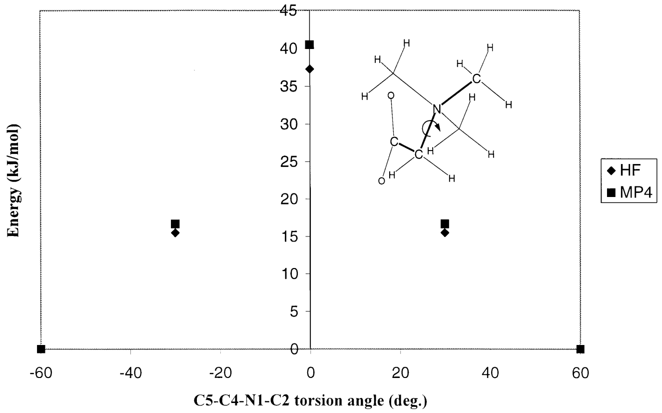

Fig. 4. Graphical energy profile of the rotational barrier of anhydrous betaine. Energies were calculated at HF/6-31+G(*d,p*) and MP4(SDQ/6-311G(*d,p*)//HF/6-31+G(*d,p*) levels

Table 2. MP2/6-31+G(*d,p*)//HF/6-31+G(*d,p*) natural population analysis (NPA) atomic charges of three optimized geometries of anhydrous betaine with the C5—C4—N1—C2 torsional angle fixed to 60° (ground state), 30° (intermediate) and 0° (transition state)[a]

Atom	C5—C4—N1—C2 torsion angle		
	60°	30°	0°
N1	−0.339	−0.335	−0.337
C1	−0.452	−0.450	−0.451
C2	−0.466	−0.464	−0.468
C3	−0.466	−0.459	−0.451
C4	−0.380	−0.362	−0.335
C5	0.727	0.719	0.699
O1	−0.755	−0.760	−0.723
O2	−0.686	−0.684	−0.723
H1	0.248	0.242	0.239
H2	0.252	0.252	0.248
H3	0.234	0.231	0.231
H4	0.243	0.256	0.281
H5	0.303	0.297	0.281
H6	0.254	0.246	0.239

[a] For the numbering of the atoms see Figs. 1 and 3

Table 3. Calculated MP2 atomic charges of betaine monohydrate in the experimental geometry and of anhydrous betaine in the MP2/6-31+G(*d,p*) optimized C_s – symmetric geometry. Values for anhydrous betaine are given in parentheses

Atom[a]	Method			
	NPA	CHELPG	MK	Mulliken
N1	−0.286 (−0.339)	0.272 (0.494)	0.371 (0.469)	−0.636 (−0.531)
C1	−0.372 (−0.452)	−0.212 (−0.328)	−0.355 (−0.433)	−0.125 (−0.200)
C2	−0.377 (−0.466)	−0.059 (−0.290)	−0.285 (−0.475)	−0.129 (−0.233)
C3	−0.379 (−0.466)	−0.053 (−0.290)	−0.229 (−0.475)	−0.133 (−0.233)
C4	−0.310 (−0.380)	−0.414 (−0.224)	−0.973 (−0.369)	−0.009 (−0.098)
C5	0.737 (0.727)	0.886 (0.798)	1.022 (0.823)	0.577 (0.400)
O1	−0.760 (−0.755)	−0.724 (−0.752)	−0.723 (−0.761)	−0.764 (−0.591)
O2	−0.715 (−0.686)	−0.713 (−0.696)	−0.730 (−0.688)	−0.695 (−0.534)
H1	0.219 (0.248)	0.093 (0.122)	0.141 (0.166)	0.159 (0.168)
H2	0.223 (0.252)	0.124 (0.127)	0.172 (0.164)	0.164 (0.177)
H3	0.213 (0.234)	0.062 (0.094)	0.127 (0.153)	0.146 (0.154)
H4	0.218 (0.243)	0.085 (0.094)	0.160 (0.153)	0.157 (0.166)
H5	0.257 (0.303)	0.085 (0.110)	0.164 (0.173)	0.221 (0.252)
H6	0.229 (0.254)	0.127 (0.175)	0.303 (0.248)	0.177 (0.178)

[a] For the numbering of the atoms see Figs. 1 and 3

Table 4. Calculated and experimental fundamental vibrations (in cm^{-1}) of C_s symmetric anhydrous betaine. Symmetries and non-zero IR intesities (in $\mathrm{km\ mol}^{-1}$) are given in parentheses

Method	Frequencies
HF/6-31+G(*d*,*p*)[a]	3372(*a*′,19) 3368(*a*″) 3331(*a*″,16) 3321(*a*′,30) 3316(*a*″,6) 3311(*a*′,6) 3308(*a*′,2) 3254(*a*′,9) 3234(*a*′,47) 3223(*a*′,7) 3223(*a*″,26) 1923(*a*′,796) 1666(*a*′,56) 1644(*a*″,22) 1639(*a*′,29) 1626(*a*″,5) 1621(*a*′,1) 1613(*a*′,37) 1598(*a*″) 1583(*a*′,2) 1571(*a*′,27) 1555(*a*″,4) 1509(*a*′,209) 1466(*a*″,19) 1466(*a*′,118) 1426(*a*′,13) 1378(*a*′,17) 1324(*a*″) 1240(*a*′,7) 1233(*a*″) 1173(*a*″,1) 1096(*a*″) 1074(*a*′,28) 1023(*a*″,48) 1013(*a*′,20) 950(*a*′,140) 831(*a*′) 772(*a*′,49) 648(*a*′,6) 576(*a*′,1) 479(*a*″) 460(*a*′,4) 393(*a*″) 375(*a*′,7) 343(*a*′,2) 321(*a*″) 296(*a*′,1) 245(*a*″,3) 238(*a*′,13) 153(*a*″,9) 65(*a*″,1)
B3LYP/6-31+G(*d*,*p*)[b]	3178(*a*′,33) 3174(*a*″,8) 3172(*a*″) 3165(*a*′,21) 3161(*a*″,5) 3158(*a*′,19) 3153(*a*″,3) 3089(*a*′,11) 3072(*a*′,51) 3065(*a*′,20) 3061(*a*″,25) 1766(*a*′,568) 1548(*a*′,47) 1525(*a*″,14) 1511(*a*′,30) 1504(*a*″,8) 1500(*a*′,2) 1475(*a*″) 1473(*a*′,9) 1452(*a*′,4) 1438(*a*′,38) 1414(*a*″,12) 1343(*a*′,81) 1332(*a*″,5) 1329(*a*′,140) 1290(*a*′,1) 1253(*a*′,8) 1211(*a*″,2) 1134(*a*′,5) 1130(*a*″) 1076(*a*″,1) 991(*a*″,1) 981(*a*′,18) 929(*a*″,24) 876(*a*′,30) 855(*a*′,89) 763(*a*′,1) 696(*a*′,42) 583(*a*″,6) 526(*a*′) 448(*a*″) 430(*a*′,5) 363(*a*″,1) 344(*a*′,7) 320(*a*′,1) 304(*a*″) 297(*a*′,1) 236(*a*″,1) 222(*a*′,11) 152(*a*″) 66(*a*″)
Experimental[c]	3397, 3048, 3017, 2964, 2943, 1631, 1498, 1483, 1458, 1415, 1383, 1336, 1298, 1240, 1143, 1010, 984, 952, 935, 893, 714, 592, 545

[a] When compared to experimental frequencies, these values must be multiplied by 0.89 to eliminate systematic errors [30]

[b] When compared to experimental frequencies, these values must be multiplied by 0.96 to eliminate systematic errors [30]

[c] From Ref. [5]

tal and calculated frequencies of the C_s symmetric ground-state anhydrous betaine are shown in the Table 4. Since all HF and B3LYP frequencies of the optimized geometry are positive, the structure is confirmed to be an energy minimum.

4 Conclusions

The present calculations explain why betaine preferentially crystallizes in a highly symmetric form. The local C_s symmetry of the betaine molecule is in part a result of weak electronic interaction, an internal hydrogen bond, resulting in slight charge transfer between the methyl hydrogens H5 and H5' and the carboxylic oxygen O1 as the analysis of NPA charges indicates. Experimental and calculated structural parameters are in agreement, but they do not alone give a definitive answer to the question concerning the weak intramolecular hydrogen bonding.

The calculated rotational barrier of the carboxylic group is 40.5 kJ/mol at the MP4(SDQ)/6-311G(*d*,*p*)// HF/6-31+G(*d*,*p*) level of theory. This high C—C single-bond rotational barrier is consistent with the breaking of the internal hydrogen bonds O1—H5 and O1—H5′ which stabilize the ground-state C_s structure. Notable structural change, shortening of about 50 pm in the length of the molecule in its eclipsed transition-state and C_s ground-state conformations, partly contributes to the high rotational barrier.

Acknowledgements. The financial assistance of Cultor Oy, Finnsugar Bioproducts, and a computational grant from the Center for Scientific Computing (Finland) are acknowledged.

References

1. Ilczyszyn MM, Lis T, Ratajczak H (1995) J Mol Struct 372: 9
2. Baran J, Drozd M, Glowiak T, Sledz M, Ratajczak H (1995) J Mol Struct 372: 131
3. Kruip S, Schaak G, Schmitt-Lewen M (1992) Phys Rev Lett 68: 496
4. Cayley S, Lewis BA, Record MT (1992) J Bacteriol 174: 1586
5. Viertorinne M, Mathlouthi M, Valkonen J, Pitkänen I, Nurmi J (1998) J Mol Struct (accepted)
6. Toccalino PL, Harmon KM, Harmon JJ (1988) J Mol Struct 189: 373
7. Latajka Z, Ratajczak H (1995) Bull Pol Acad Sci Chem 43: 103
8. Stewart JJP (1989) J Comput Chem 10: 209
9. Stewart JJP (1989) J Comput Chem 10: 221
10. Hypercube Inc (1994–1995) HyperChem 4.5 for Windows
11. Frisch MJ, Trucks GW, Schlegel HB, Gill PMW, Johnson BG, Robb MA, Cheeseman JR, Keith T, Petersson GA, Montgomery JA, Raghavachari K, Al-Laham MA, Zakrzewski VG, Ortiz JV, Foresman JB, Cioslowski J, Stefanov BB, Nanayakkara A, Challacombe M, Peng CY, Ayala PY, Chen W, Wong MW, Andres JL, Replogle ES, Gomperts R, Martin RL, Fox DJ, Binkley JS, Defrees DJ, Baker J, Stewart JP, Head-Gordon M, Gonzales C, Pople JA (1995) Gaussian 94 revision D.4. Gaussian, Pittsburgh, Pa
12. Hariharan PC, Pople JA (1974) Theor Chim Acta 28: 213
13. Becke AD (1993) J Chem Phys 98: 5648
14. Lee C, Yang W, Parr RG (1988) Phys Rev B 37: 785
15. Miehlich B, Savin A, Stoll H, Preuss H (1989) Chem Phys Lett 157: 200
16. Møller C, Plesset MS (1934) Phys Rev 46: 618
17. Saebo S, Almlöf J (1989) Chem Phys Lett 154: 83
18. Frisch MJ, Head-Gordon M, Pople JA (1990) Chem Phys Lett 166: 275
19. Frisch MJ, Head-Gordon M, Pople JA (1990) Chem Phys Lett 166: 281
20. Williams DE, Yan JA (1988) Adv At Mol Phys 23: 87
21. Reed AE, Weinstock RB, Weinhold F (1985) J Chem Phys 83: 735
22. Reed AE, Curtiss LA, Weinhold F (1988) Chem Rev 88: 899
23. Breneman CM, Wiberg KB (1990) J Comput Chem 11: 361
24. Singh UC, Kollman PA Jr (1984) J Comput Chem 5: 129
25. Besler BH, Merz KM, Kollman PA Jr (1990) J Comput Chem 11: 431
26. Molecular Simulations Inc. (1997) WebLab Viewer, version 2.01
27. Szafran M, Koput J (1996) J Mol Struct 381: 157
28. Goodman L, Leszczynski J, Kundu T (1994) J Phys Chem 100: 1274
29. Jeffrey GA, Mitra J (1983) Acta Crystallogr B39: 469
30. Foresman JB, Frisch AE (1996) Exploring chemistry with electronic structure methods, 2nd edn., Gaussian, Pittsburgh, Pa
31. Hehre WJ, Radom L, Schleyer PvR, Pople JA (1986) Ab initio molecular orbital theory. Wiley, New York, p 264
32. Cason CJ (1991–1997) POV-Ray for Windows, version 3.02